Chemical kinetics model for hypoxia effect in the afterglow of an argon plasma jet

J van Der Paal, S Heijkers, J Slaets, G Busco, E Robert, J.-M Pouvesle, A Bogaerts

Chemical kinetics model for hypoxia effect in the afterglow of an argon plasma jet

J. Van der Paal[1], S. Heijkers[1], J. Slaets[1], G. Busco[2,3], E. Robert[3], J.-M. Pouvesle[3] and A. Bogaerts[1]

[1]*Research group PLASMANT, Department of Chemistry, University of Antwerp, Belgium*
[2]*CBM, UPR 4301 CNRS Orléans, France*
[3]*GREMI, UMR 7344 CNRS-Université d'Orléans, France*

Abstract: In the present study, we investigate the plasma chemistry in the afterglow of an argon plasma jet, by means of a chemical kinetics model. More specifically, we focus on the effect of a depleting oxygen fraction in the afterglow surroundings. Indeed, i*n vitro*, this is induced by the argon flow during plasma treatment, but moreover, this also occurs *in vivo* in the surroundings of cancer cells. Our simulations indicate that the alterations of the density of biomedically important RONS strongly depend on the origin of each species.

Keywords: Chemical kinetics, argon plasma jet, afterglow chemistry, hypoxia, RONS.

1. Introduction

In the field of plasma oncology, cold atmospheric plasmas are used as a cancer treatment modality. The main advantage over traditional therapies, is that CAPs are able to selectively induce cell death in cancer cells while leaving their healthy counterparts far more unharmed. The underlying mechanisms remain, however, elusive [1]. To increase the knowledge of the processes which occur upon interaction of the afterglow of CAPs with cells or tissues (both *in vitro* and *in vivo*) it is important to identify the main species that are capable of reaching these cells. This knowledge would allow us (i) to estimate the possible interactions/reactions which might occur, and (ii) to fine tune plasma parameters (concerning both the plasma source as well as the carrier gas).

Multiple studies have already reported the reaction chemistry of the afterglow of atmospheric plasma jets (e.g. [2-4]). However, none of these studies has implemented the hypoxia effect (decreased O_2-fraction in cellular microenvironment) which occurs upon treating cells *in vitro* [5] and which is also of key importance for *in-vivo* treatment of cancer cells. Indeed, it is known that due to the rapid growth of tumorous tissue, large portions of a solid tumour are surrounded by hypoxic microenvironments. This hypoxic microenvironment is the result of the outermost cancer cells, consuming nearly all the available oxygen in order to proliferate more rapidly. Therefore, in the present work, we study the afterglow of an argon atmospheric pressure plasma jet (APPJ), investigating the effect of a decreasing molecular oxygen fraction on the plasma chemistry.

2. Computational method

We used the ZDPlaskin 0D chemical kinetics model [6] combined with the built-in BOLSIG+ Boltzmann-solver [7]. The chemistry-set used in this study is largely taken from Murakami et al. [4]. However, to include additional relevant biomedically active species (e.g. H_2O_2, HO_2, HNO_3 or HNO_2), we extended this chemistry set with the reactions describing the behaviour of these species, adopted from the chemistry set of Van Gaens et al [2]. The profiles of the applied power density, gas flow velocity and molecular oxygen density in the afterglow are fitted to experimental data [8,9]. Using our 0D chemical kinetics model, the density profiles of various biomedically relevant species are calculated and the effect of the molecular oxygen fraction in the afterglow on these profiles is evaluated.

3. Results

To mimic a plasma jet that is used in medical applications, the gas temperature in the afterglow was fixed at room temperature (*i.e.* 300K). To study the hypoxia effect, which is induced by the gas flow of the plasma jet, the gas flow rate was varied, ranging from 1 up to 5 slm. The effect of this flow rate on the molecular oxygen density in the afterglow is illustrated in Figure 1. In the model used, ambient air diffusion into the afterglow region only starts 0.12 cm after the nozzle exit, which can also been derived from Figure 1. The density profiles of molecular nitrogen and water, also present in the ambient air (with a relative humidity of 50%), are very similar.

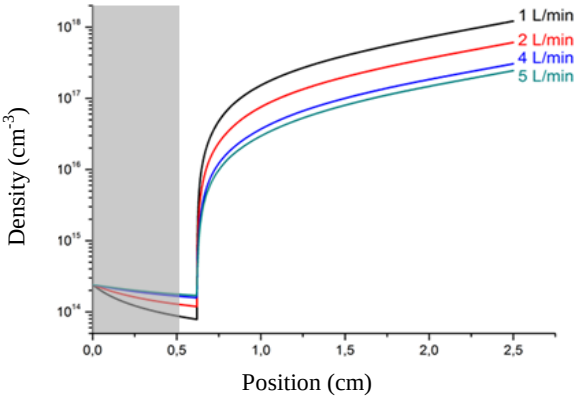

Figure 1: Effect of the gas flow rate on the molecular oxygen (O_2) density in the afterglow. The grey zone indicates the region inside the plasma jet.

Upon increasing the flow rate, different trends can be observed for different biomedically active species. As expected, the density of most of the species decreases if the flow rate increases, which can be seen in Figure 2 for N_2O, NO, O_3, HNO_3 and HNO_2. This can be explained by the O_2 and N_2 densities for these conditions (see Figure 1). Indeed, all relevant biomedical species contain either oxygen or nitrogen, or both (these are the so-called Reactive Oxygen and Nitrogen Species, *i.e.*, the RONS) and thus, they require molecular oxygen and nitrogen to be generated. Therefore, due to the decreasing O_2 and N_2 fraction (upon increasing the flow rate), the fraction of these species also decreases.

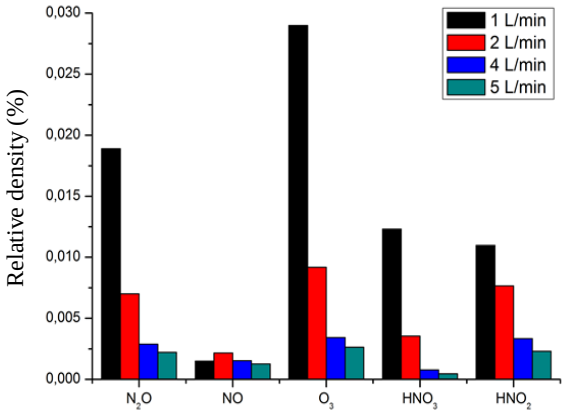

Figure 2: Density of N_2O, NO, O_3, HNO_3 and HNO_2 at a position of 2.5 cm, normalized against the total gas density (the values of N_2O are multiplied by a factor of 10, to make the differences more visible).

For a number of other species, however, the opposite trend can be observed. Indeed, the density of O, O^-, O_2^-, OH, H, HO_2, N and NO_3^- increases upon increasing the gas flow rate, which is illustrated in Figure 3 for O radicals, as a representative example for all of the species mentioned.

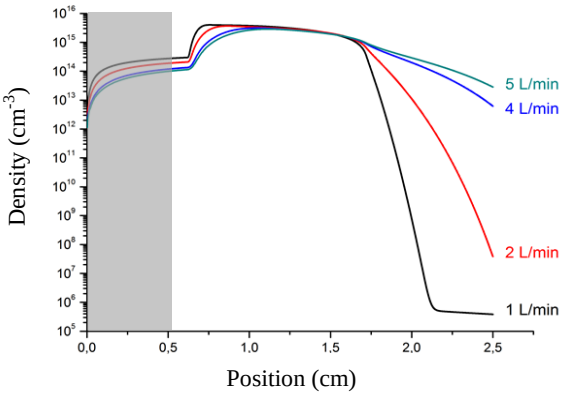

Figure 3: Effect of the gas flow rate on the density profile of O radicals.

This contradictory trend can be explained by looking at the electron density profile upon varying the flow rate, which is illustrated in Figure 4.

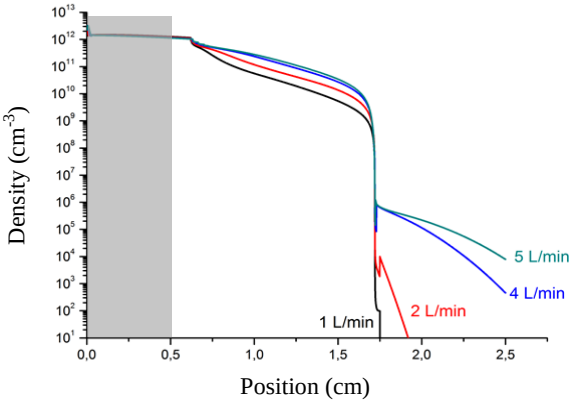

Figure 4: Effect of the gas flow rate on the electron density profile.

Indeed, from Figure 4, it is clear that upon increasing the gas flow rate, the electron density decreases less drastically when the power density (and thus the reduced electric field) is reduced to zero (which occurs at a position of 1.76 cm). As some of the species mentioned above (*i.e.*, N, O, O^-, and OH) are mainly generated due to electron impact reactions, their density increases if the electron density increases (which is the case for higher gas flow rates). Other species (*e.g.*, H, HO_2, O_2^-), on the other hand, are mainly generated due to reactions involving O or OH radicals. Therefore, if the densities of these radicals increase upon increasing the gas flow rate (see Figure 3), the density of the species they generate also increases.

Finally, the density of H_2O_2 shows a different behaviour from the trends discussed above. Indeed, upon increasing the gas flow rate, the density of H_2O_2 decreases in the first part of the afterglow, but increases in the second part of the afterglow (the second part of the afterglow starts when

the power density drops to zero, at a position of 1.76 cm). This is illustrated in Figure 5.

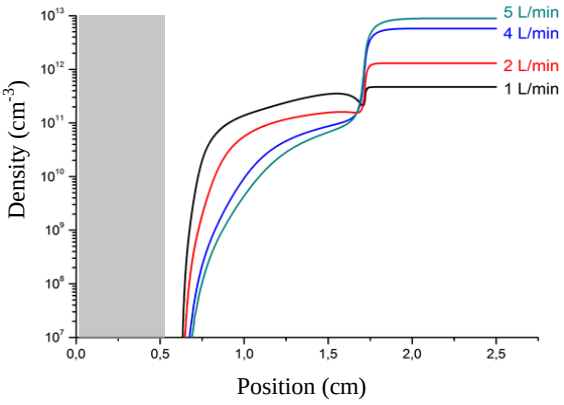

Figure 5: Effect of the gas flow rate on the density profile of hydrogen peroxide (H_2O_2)

The density profile of H_2O_2 upon increasing the gas flow rate can be explained by looking at Figures 3 and 4. The most important loss reaction of H_2O_2 is electron impact dissociation:

$$e^- + H_2O_2 \rightarrow H_2O + O^- \quad (1)$$

As can be seen from Figure 4, the electron density is higher at higher flow rates. Therefore, the reaction rate of this loss process will be higher, and thus, the density of H_2O_2 will be lower in this first region. The main production term for H_2O_2 on the other hand, is the recombination reaction of two OH radicals:

$$OH + OH + Ar \rightarrow H_2O_2 + Ar \quad (2)$$

Because OH radicals follow the same trend as O radicals (illustrated in Figure 3), their density will be much higher in the second part of the afterglow, upon increasing the flow rate. Therefore, in this region, the production rate of H_2O_2 will be much higher, overcompensating for the decreasing electron density in this region, resulting in a net increase of the H_2O_2 density in the second part of the afterglow.

4. Conclusions

In this study, we have modelled the plasma chemistry in the afterglow of an argon plasma jet, using a zero-dimensional chemical kinetics model. More specifically, we focused on the hypoxia effect (*i.e.* a depletion of the molecular oxygen concentration), which occurs *in vitro* when ambient air is blown away due to the plasma carrier gas, and which is also important in the microenvironment of solid tumours *in vivo*.

Our results indicate that, upon increasing the gas flow rate of the plasma, the molecular oxygen fraction decreases in the afterglow. This, in turn, leads to the up- or down-regulation of some of the biomedically important reactive oxygen and nitrogen species (RONS). Indeed, the concentration of e.g. N_2O, NO, O_3, HNO_3 and HNO_2 decreases upon increasing the gas flow rate, which is caused by the decreasing O_2 and N_2 fraction in the afterglow (as these are required for the generation of the species mentioned). The density of other RONS, including O, O^-, O_2^-, OH, H, HO_2, N and NO_3^-, on the other hand, increases by increasing the gas flow rate, which is due to an increasing electron density at these higher flow rates. Finally, the density of H_2O_2 first decreases by increasing the gas flow rate, due to more prominent loss by electron impact dissociation, but increases again more drastically at these higher flow rates at longer distances from the nozzle exit, due to recombination of 2 OH radicals, which become more important at higher flow rates.

In general, the results of our model indicate (i) that the density of biomedically active species strongly depends on the gas flow rate and (ii) that the behaviour at different flow rates depends on the production (and loss) reactions of each species. Moreover, for some species (such as hydrogen peroxide), the effect of the gas flow rate depends also on the distance from the nozzle exit. This indicates that, in experimental set-ups, the distance to the sample that is being treated is a critical factor.

5. Acknowledgements

The authors acknowledge financial support from the Fund for Scientific Research (FWO) Flanders, grant number 11U5416N. The calculations were performed in part using the Turing HPC infrastructure of the CalcUA core facility of the Universiteit Antwerpen, a division of the Flemish Supercomputer Center VSC, funded by the Hercules Foundation, the Flemish Government (department EWI) and the Universiteit Antwerpen.

Furthermore, the authors acknowledge financial support from ARD2020 COSMETOSCIENCE, project PlasCosm.

6. References

[1] D. B. Graves, Plasma Process. Polym. **11**, 1 (2014)
[2] W. Van Gaens, A. Bogaerts, J. Phys. D: Appl. Phys. **46**, 275201 (2013).
[3] A. Schmidt-Bleker, J. Winter, S. Iseni, M. Dunnbier, K.D. Weltmann and S. Reuter J. Phys. D: Appl. Phys. **47**, 145201 (2014).
[4] T. Murakami, et al., Plasma Sources Sci. Technol. **22**, 015003 (2013).
[5] C. Douat et al., IWPCT3, Washington, 2016
[6] S. Pancheshnyi, B. Eismann, G.J.M. Hagelaar and L.C. Pitchford, Computer code ZDPlasKin (2008).
[7] G.J.M. Hagelaar and L.C. Pitchford, Plasma Sources Sci. Technol. **14**, 722 (2005).
[8] S. Hofmann, A.F.H. van Gesse, T. Verreycken and P. Bruggeman, Plasma Sources Sci. Technol. **20**, 065010 (2011).
[9] D. Ellerweg, A. von Keudell and J. Benedikt, Plasma Sources Sci. Technol. **21**, 034019 (2012.